Point Cloud Generation by Gimbal-mounted LiDAR and Multi-directional Camera for Lunar Surveying

Rikako Shigefuji. [1*], Masafumi Nakagawa.[1], Keitaro Kitamura.[2], Masanori Takigawa.[2] and Taizo Kobayashi.[3]

[1]Shibaura Institute of Technology, Japan

[2]Asia Air Survey Co.,Ltd,, Japan

[3]Ritsumeikan University, Japan

*ah19029@shibaura-it.ac.jp

Abstract: *In recent years, research activities related to the development of the lunar surface, such as the Artemis project, have progressed. However, it is not easy to survey the lunar surface using conventional surveying instruments such as a total station due to the lack of reference points, non-GNSS environments, extreme temperature difference, cosmic radiation, and lower gravity. In addition, conventional image-based measurement and SLAM (Simultaneous Localization and Mapping) are also difficult due to a sandy surface covering the lunar surface, called as the regolith. On the other hand, lunar construction requires more efficient work with digital twinning to improve construction and transportation costs. Therefore, we have developed a point cloud acquisition method (LiDAR-SfM/MVS) that combines marker-based LiDAR-SLAM for reference point measurement and SfM/MVS processing for dense point cloud acquisition. In this research, two types of measurement approaches were investigated. The first approach was a LiDAR-SfM/MVS methodology that combines SfM/MVS with multi-directional cameras and a LiDAR with an attitude heading reference system (AHRS). The second approach was SfM/MVS with multi-directional cameras and a LiDAR mounted on a 3-axis gimbal. Both approaches acquire asynchronous images with a multi-directional camera to achieve 3D measurements even in environments with poor geometric and color features, such as the lunar surface. The asynchronous images are combined and processed to generate SfM point clouds, and the generated point clouds are registered with the marker positions obtained from the LiDAR point clouds to obtain with scale information. Our experiments were conducted in two types of simulated lunar surface environments. We have confirmed that even in a poor environment such as the lunar surface, it is possible to acquire point clouds of the ground surface with the accuracy of approximately 0.04[m] by using LiDAR combined with AHRS, or by measuring from a gimbal-mounted LiDAR mounted on a 3-axis gimbal and images from a multi-directional camera, even in black or white colored ground surfaces.*

Keywords: Lunar Survey, Point Clouds, LiDAR-SLAM, SfM/MVS

Introduction

In recent years, research activities related to lunar exploration have been intensified through the Artemis Project, a lunar exploration project led by NASA. In Japan, R&D related to space development projects is also being promoted under the Strategic Program for Acceleration of Space Utilization. In Japan, i-Construction, which aims to improve productivity by introducing ICT technology to construction sites, is being promoted, and

unmanned construction technology is being developed to alleviate labor shortages at construction sites. There is a growing movement to apply these remote and automated construction technologies developed on the ground to space exploration. However, the lunar surface is difficult to work on manually due to extreme temperature differences and space radiation, and construction and transportation costs require even less rework than construction on the ground. For this reason, it is necessary to develop digital twins and topographic data for lunar construction simulation. It is difficult to apply conventional surveying methods such as Global Navigation Satellite System (GNSS) and total station to the lunar surface. Moreover, it is not easy to apply conventional imaging methods to the lunar surface, because the lunar surface is covered with a sandy surface called regolith (Charles,2003). The regolith is a difficult surface for conventional imaging methods, and the microtopography and non-GNSS environment make it extremely difficult to apply conventional simultaneous localization and mapping (SLAM) and mobile mapping system measurements. Therefore, we develop a point cloud acquisition method (LiDAR-SfM/MVS) that combines marker-based LiDAR-SLAM for reference point measurement and SfM/MVS processing for high-density point cloud acquisition (Shigefuji et al., 2023). In this study, we use LiDAR with an attitude heading reference system (AHRS) or LiDAR mounted on a 3-axis gimbal (gimbal-mounted LiDAR) and asynchronous images taken by a multi-directional camera to provide redundant 3D measurements even in poor environments such as the lunar.

Literature Review

There have been many developments in lunar positioning and technology. For example, a method using Visual-SLAM to map the autonomous motion of a lunar rover was investigated (Pei et al.,2002). Here, features were extracted using ORBs to identify the camera position, and a point cloud map was created using triangulation of the multi-view geometry. The accuracy of feature point extraction was improved by applying the grid extraction method to lunar images with little texture. Although the use of visual sensors has advantages such as low cost and low power consumption, it is difficult to estimate the attitude by camera in the lunar environment where the illumination environment tends to change. The mapping and positioning accuracy of LiDAR-SLAM has been verified in a simulated lunar environment (Du, et al., 2022). Because the lunar surface is an environment where illumination changes rapidly and the terrain is complex, limiting the

computational capability of intelligent guidance systems, the SLAM algorithm, which is not affected by illumination and other factors, was used for verification. To reduce the computational cost of the SLAM algorithm, the frontend uses an algorithm that detects scenes with large feature points by calculating the curvature of the point cloud is used at the frontend, the point clouds are replaced. At the backend, a factor-graph optimization methodology is used to reduce the cumulative error. Crater detection using LiDAR has also been performed for lunar rover path planning and safe travel (Yier et al., 2023), based on the DBSCAN and RANSAC crater detection and augmentation algorithms. The algorithm has been validated in a simulated experimental environment. Since craters are more difficult to detect as they approach than normal three-dimensional obstacles, range errors and vertical angle errors were identified as factors affecting the probability of crater detection.

Methodology

The methodology proposed in this study is shown below (Figure 1). LiDAR data and camera images are used as input data and output as colored dense point clouds and sensor position data, consisting of LiDAR point cloud acquisition, marker center extraction from the LiDAR point cloud, SfM/MVS processing, and registration with the SfM/MVS point cloud (LiDAR-SfM/MVS).

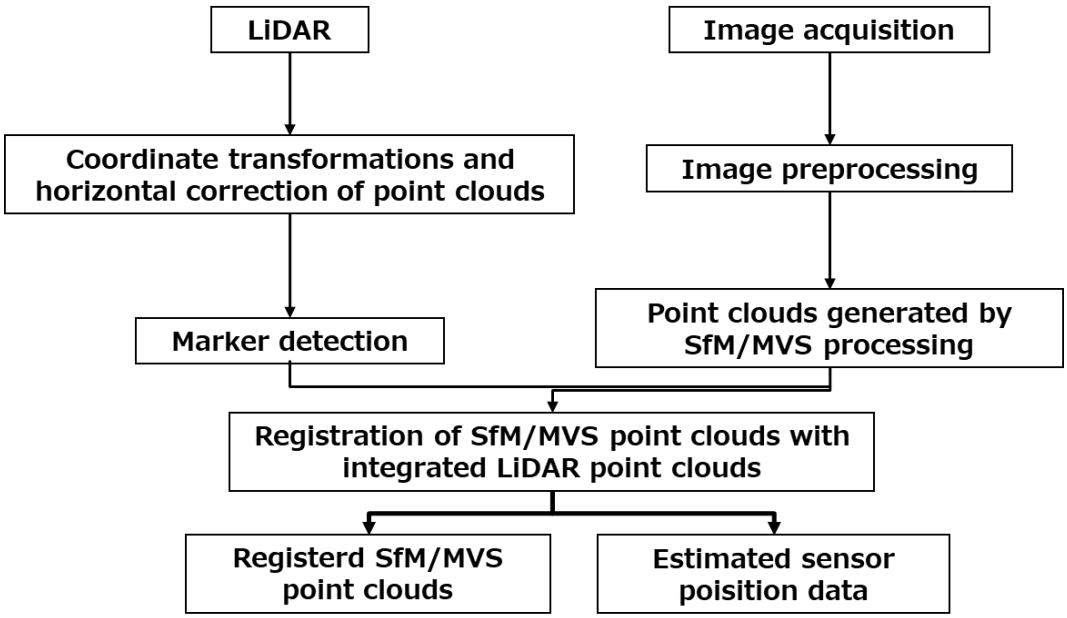

Figure 1: Methodology.

a. LiDAR point cloud acquisition:

For LiDAR measurements, measurements from LiDAR combined with AHRS or gimbal-mounted LiDAR are used. In the case of LiDAR combined with AHRS, the roll, pitch, and yaw angles obtained from the AHRS are used to correct for rover motion. The horizontally corrected laser scan data is integrated and used as the input point cloud for the marker extraction process. When using gimbal-mounted LiDAR is applied, the point cloud registered based on the gimbal rotation angle is used as the input point cloud for the marker extraction process.

b. Marker extraction from point clouds

The extraction of markers from the LiDAR point clouds is performed after the LiDAR point clouds are converted to voxels. The voxel height direction is used to classify the ground surface and the marker points. After selecting the approximate location of the marker, a sphere model is fitted to the marker point cloud to estimate the center location of the marker and generate a marker point cloud with uniform point density.

c. SfM/MVS processing:

To generate point clouds with SfM/MVS processing, it is necessary to take clear images to obtain enough feature points even in a feature-poor environment such as the lunar surface. For this purpose, a high-resolution camera with a large sensor size and bright lens was used. In addition, the camera was set up in four directions (front, back, left, right, and diagonally down at 45° downward) to ensure stable imaging of the lunar surface.

d. Registration of SfM/MVS point clouds:

Since the point clouds generated by SfM/MVS alone lack scale information, this study obtains scale information from the point clouds generated by LiDAR-SLAM. The point clouds with scale information are generated as LiDAR-SfM/MVS processing by aligning the point clouds acquired by SfM/MVS processing with the marker point clouds (spherical point clouds) acquired by LiDAR-SLAM processing. First, due to the difference in coordinate systems, there is a large initial positional discrepancy between the LiDAR point cloud and the SfM point cloud, and the first registration is performed to correct for this. The second registration uses the marker size obtained from the scale adjustment in

the first registration is used for more accurate registration. The second registration uses the marker size obtained from the scale adjustment made in the first registration.

e. Scan matching point clouds:

Scan matching is the process of registering two sets of point clouds and matching the shapes in the two sets of point clouds. The Iterative Closest Points (ICP) algorithm (Szymon et al., 2001) is used for scan matching in SLAM in this study. The ICP algorithm can provide highly accurate registration of noiseless point clouds based on the least squares method. However, when matching point clouds that contain measurement noise and have low range accuracy, this leads to an increase in the accumulation error generated by SLAM. In this study, we improve the performance of point cloud scan matching by incorporating a spherical object recognition process into LiDAR-SLAM.

Experiment

Experiments were conducted in two environments: a lunar surface simulation environment and a simulated ground experiment.

a. Experiments in a simulated lunar environment:

The experiment was conducted in a Lunar Survey Field (in the Space Exploration Laboratory at JAXA's Sagamihara Campus), which simulates the lunar survey (Figure 2). The regolith was simulated with silica sand, and xenon lamps were installed as a pseudo-sun to conduct a rover driving experiment. The field consisted of a flat area and a hilly area to simulate the topography of the lunar surface. Seven red spherical markers with a diameter of 0.20[m] were placed on the field for the experiment. In addition, red spherical markers with a diameter of 0.30 [m], cubic markers, and white markers were placed as test markers. A teleoperated autonomous mobile robot (Multi Crawler Robot, JAXA) was used as a rover to drive and measure between the equally spaced markers. LiDAR (VLP32-C, Velodyne) and AHRS (MTi-G-710, Xsens) were mounted on the top panel of the autonomous mobile robot (0.30[m] above the ground), and four high-resolution cameras (DSC-RX0M2, SONY) were mounted at the front, back, left and right (Figure 3, Table 1). was used for data acquisition at 10 Hz and AHRS at 100 Hz. The camera was mounted at a height of 1.5[m] above the ground, looking down at an angle of 45° to

capture images of the ground surface. Because target data acquisition is necessary for scale factor estimation, the rover moved back and forth along two paths between markers.

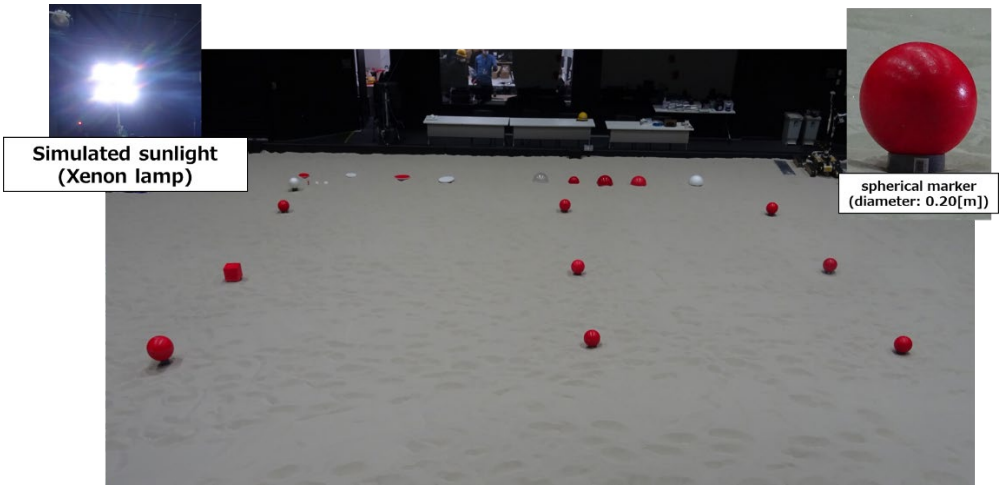

Figure 2: Experiment field.

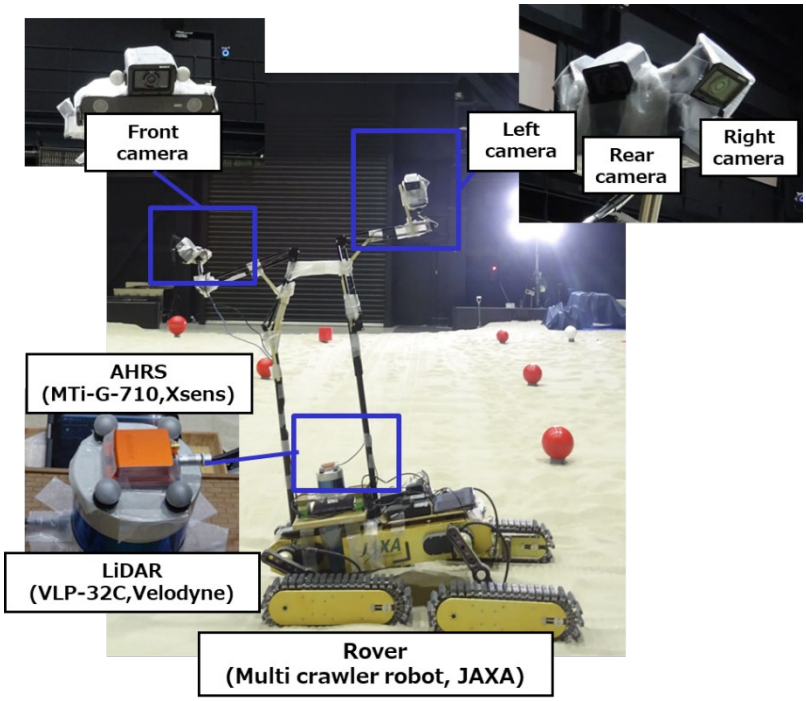

Figure 3: 3D measurement system.

Table 1: Sensor specifications.

High Resolution Camera(DSC-RX0M2,SONY)	
The number of pixels	15.3 milion pixels
Frame rate	1fps
Focus mode	Auto
AHRS(MTi-G-710,Xsens)	
Angle resolution/Roll	0.2°
Angle resolution/Pitch	0.3°
Angle resolution/Yaw	0.8°
Sampling rate	100Hz
LiDAR(VLP-32C,Velodyne)	
Measurement range	200m
Range accuracy	Up to ±3cm
Horizontal field of view	360°
Vertical field of view	40°
Sampling rate	10Hz

b. Simulated ground experiment:

The experiments were conducted in an experimental field simulating the lunar environment on the Biwako Kusatsu Campus of Ritsumeikan University. The field was a black site for soil and ground investigation, with red spherical markers of 0.20 [m] diameter at 14 points on the field. The rover was equipped with a LiDAR (VLP16, Velodyne), four industrial cameras (DFK33UX264, The Imaging Source) with 1.0-inch CMOS sensors (front, rear, left, and right), and a soil and subsoil investigation system consisting of a radioisotope moisture density meter and load and shear test tools (The system consists of radioisotope moisture density meters, loading and shear test tools (Figure 4, Table 2). Measurements were taken while the rover was masking ground measurements on the 5 lanes x 7 ground measurement points in the field. The LiDAR was rotated 360° by using a gimbal to take measurements.

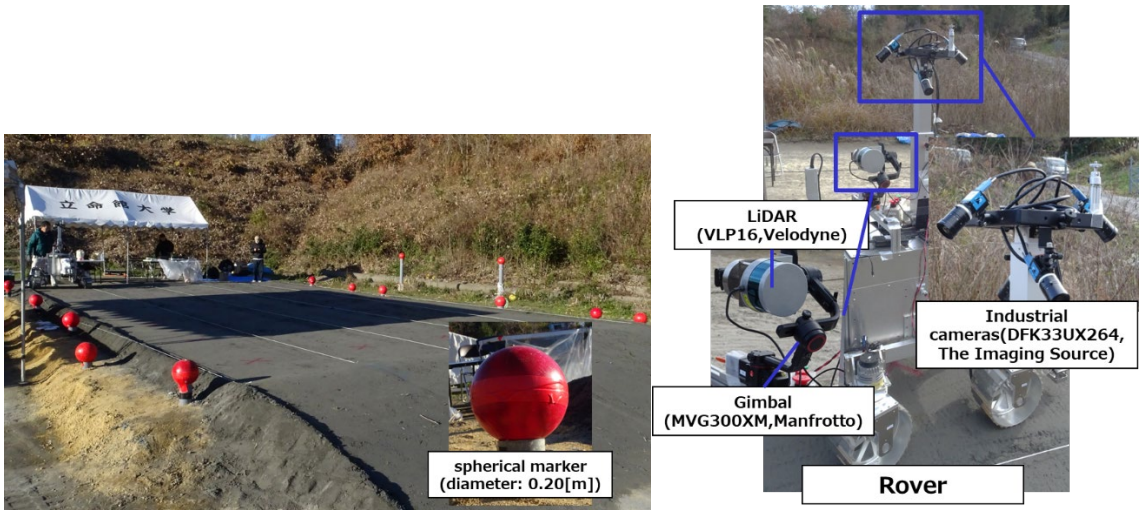

Figure 4: Experiments field and 3D measurement system.

Table 2: Sensor specifications.

Industrial cameras(DFK33UX264,The Imaging Source)	
The number of pixels	15.3 milion pixels
Frame rate	1fps
Focus mode	Auto
Gimbal(MVG300XM,Manfrotto)	
Maximum tilt angle	340°
Maximum roll angle	340°
Maximum pan angle	360°
LiDAR(VLP-16,Velodyne)	
Measurement range	100m
Range accuracy	Up to ±3cm
Horizontal field of view	360°
Vertical field of view	40°
Sampling rate	10Hz

Results

a. Experimental results in a simulated lunar environment:

The SfM/MVS point cloud was output from the images acquired by driving the rover with the light source behind it (Figure 5). Out of a total of 665 images taken, 302 blur-free images were used as input for the SfM/MVS processing. The results show that a high-density point cloud data of the ground surface can be obtained by using high-resolution camera even for a white measurement target with few shape features, such as a sand surface. Although there were some missing points in the shadows of markers and at the periphery of the field, it was confirmed that the point clouds were generated uniformly around the path traveled by the rover. The registration results of the SfM point cloud using the marker point clouds extracted from LiDAR and the marker extraction results obtained from LiDAR are shown below (Table 3). Table 3 shows that the residuals of the LiDAR and SfM point clouds can be registered with the same accuracy as the LiDAR ranging accuracy (approximately 0.03 [m]), and that the voxelization of the point clouds as a pre-processing step for the sign extraction from the LiDAR point clouds reduced the point density.

Table 3: Registration results of SfM point clouds using markers extracted from LiDAR point clouds.

The number of split faces	Point cloud density [points/m^3]	Error values [m] (RMSE)
900	7.65×10^3	0.023
100	0.962×10^3	0.027
29	0.509×10^3	0.031
25	0.286×10^3	N/A

b. Results of point clouds acquired in the simulated ground experiment:

Out of 5747 images acquired by an industrial camera, input point clouds were generated by using 841 images as input data to SfM/MVS (Figure 6). The results of the simulated ground experiment confirmed that point clouds can be acquired even for black compacted ground surfaces with few geometric features, as sufficient image features could be extracted. Figure 7 shows that it is possible to detect markers from the point clouds generated by the gimbal-mounted LiDAR.

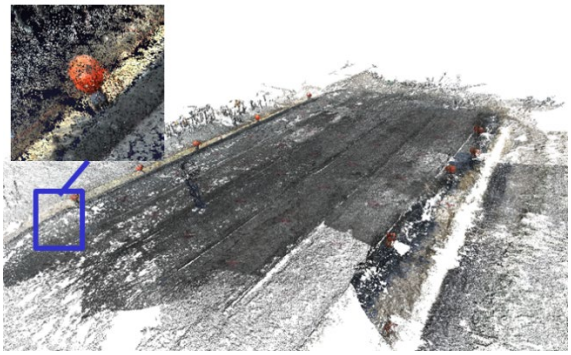

Figure 6: SfM/MVS point clouds.

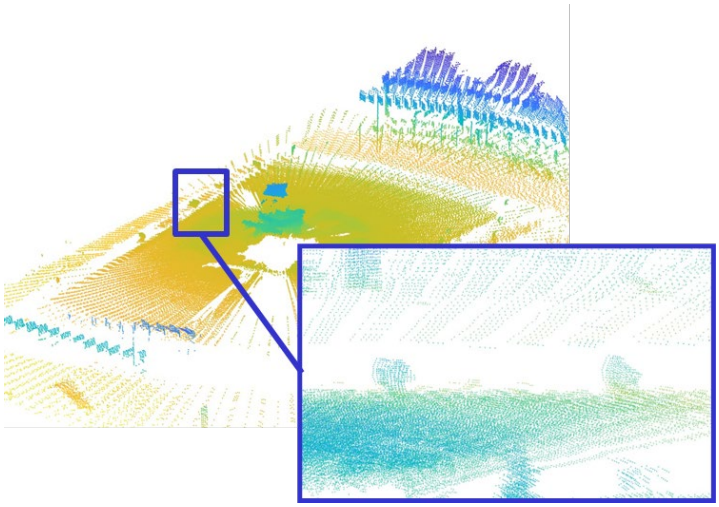

Figure 7: Gimbal LiDAR point clouds.

Discussion

The results of the lunar simulation experiment are discussed using three different trajectories (Route 1, Route 2, and Route 3) (Figure 8). Route 1 is the result of changing the direction of the rover at the turnaround point, and routes 2 and 3 are the results of switchback driving at the turnaround point. Route 3 was driven at half the speed of routes 1 and 2, and route 1 and 2 were driven at about 3 km/h. Many images were blurred due to the moving image capture in the dark environment. Therefore, only 133 of the 2102 images taken on Route 1 could be selected for SfM/MVS, and only 75 of the 1273 images taken on Route 2 could be selected for SfM/MVS. As shown in Figure 8, there were many missing points in the point cloud due to the high measurement speed and insufficient number of images as input data for SfM processing. When the measurement was performed at a low speed, blurred images and missing measurement areas were avoided, but the efficiency of image acquisition deteriorated. Although both spherical and cubic markers were extracted from the LiDAR point cloud, it was confirmed that the spherical marker was more suitable than the cubic marker when combined with LiDAR-SLAM and SfM/MVS processing. Given the white terrain of the regolith-covered lunar survey and the LiDAR measurements, red markers, which are more prominent than white or black, were considered appropriate as feature points.

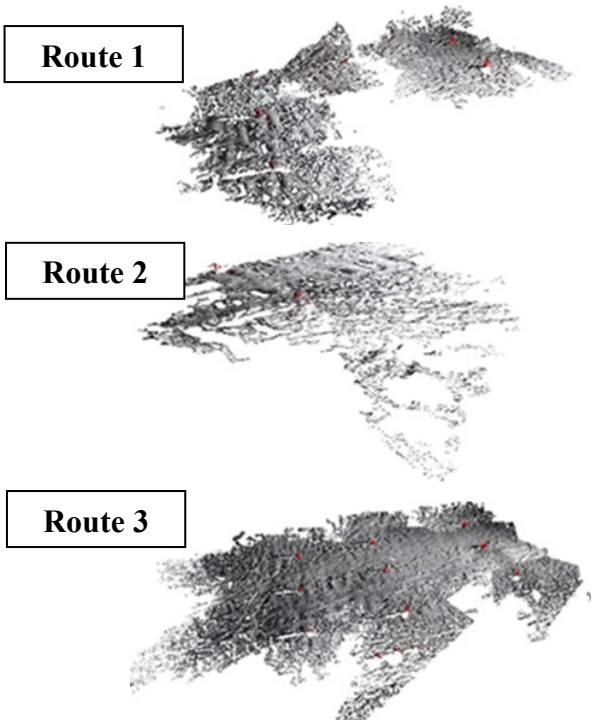

Figure 8: SfM/MVS results for each route.

Conclusion

In this study, we investigated LiDAR-SfM/MVS as a topographic surveying methodology for lunar surface development. A rover-mounted gimbal LiDAR and an asynchronous multi-directional camera were used to generate point clouds. We confirmed that even in a poor measurement environment such as the lunar surface, it is possible to acquire point clouds of the ground surface, even in black or white, by using LiDAR in combination with AHRS or by using measurements from a gimbal-mounted LiDAR mounted on a 3-axis gimbal and created by a multi-directional camera. In addition, through experiments on a simulated lunar surface, we confirmed that point cloud acquisition is possible through LiDAR-SfM/MVS processing using red spherical markers. Future works include the development of space specifications for the sensor system (durability against rocket launch and improvement of weathering performance to enable lunar surface measurements).

Acknowledgments

This research was supported by the MLIT R&D Program for the Project of Technological Innovation for Construction on Space Field.

References

Charles, M. (2003). The Lunar Petrographic Thin Section Set, pp.46-48.

Rikako Shigefuji, Karin Noguchi, Masanori Takigawa, Keitaro Kitamura, Takahiro Hiramatsu, Taizo Kobayashi, & Masafumi Nakagawa. (2023). 6 pages. Asian Conference on Remote Sensing 2023 (ACRS2023). Acquisition of Dense Point Clouds with LiDAR-SfM/MVS Lunar Environment.

Pei An, Yanchao Liu, Wei Zhang, & Zhaojun Jin. (2003). p.487-493. Vision and Computing. Vision-Based Simultaneous Localization and Mapping on Lunar Rover, International Conference on Image.

Shi Biao Du, Xin Zhao, & Hong Yong Fu. (2022). Volume 2364. AAME2022. 3D Mapping and Positioning Technology of Lunar Environment Based on LiDAR, Journal of Physics.

Yier Zhou, Xiaolu Li, & Baocheng Hua. (2023). p.1-9. Measurement. Crater identification simulation using LiDAR on Luna rover.

Szymon R, & Marc L. (2001). p.145-152. Efficient Variants of ICP Algorithm, Third International Conference on 3-D Digital Imaging and Modeling.